



Natural fractures characterization by integration of FMI logs, well logs and core data: a case study from the Sarvak Formation (Iran)

Amir Mazdarani¹ · Ali Kadkhodaie² · David A. Wood³ · Zohreh Soluki⁴

Received: 26 August 2022 / Accepted: 7 February 2023 / Published online: 20 February 2023
© The Author(s) 2023

Abstract

Carbonate reservoirs in Iran are the most important and main sources of oil and gas production. Hydrocarbon flow rates from carbonate reservoirs heavily rely on the development of natural fractures. This study focuses on the role of natural fractures on reservoir quality considering the Sarvak carbonate reservoir (southwest Iran) as the second most important oil reservoir of Iran. To identify small-scale fractures around the borehole walls, cores description and image logs were utilized. Due to high cost of coring, lack of orientation and low core recovery in fractured zones indirect methods based on image logs and conventional well logs were exploited for fracture characterizations. For this purpose, a complete set of well data including image logs (FMI), well-log-derived porosity and permeability data together with petrophysical logs were employed. Interpretation of image logs allows different types of natural structures such as open, vuggy, partly-filled and filled fractures, bedding planes and stylolites to be identified. Comparisons between the petrophysical-log and image-log interpretations provide useful relationships with reservoir characteristics. Neutron and sonic logs show a direct relationship with fracture porosity, while the density log displays an inverse correlation with fracture porosity. Neutron-density and neutron-sonic cross-plots show that the dominant lithology of the studied well is limestone with minor fractions of dolomite and shale. Total porosity ranges from 2 to 30%, while the contribution of secondary porosity, on average, is below 3%. Relationships between fracture-frequency diagrams and reservoir permeability show that high permeability zones are well correlated with the high frequencies of open and vuggy fractures and zones that have flowed oil and associated gas in production tests. Natural fracture characterization based on systematic and integrated interpretations of image logs and petrophysical data can play an important role in optimizing field development, resource recovery and production from the Sarvak reservoir. Once calibrated, this method also offers potential as an exploration tool.

Keywords Reservoir fractures · FMI well logs · Sarvak carbonate formation · Reservoir quality

Introduction

Carbonate reservoirs contain a large amount of oil and gas-in-place. It is estimated that 60% of the world's oil reserves and 40% of the world's gas reserves are present in these

reservoirs (Sadeq and Yusoff 2015; Lee et al. 2015; Dou et al. 2011; Esrafil-Dizaji et al. 2015; Kosari et al. 2017; Ezati et al. 2018; Gupta 2019; Wang et al. 2020). The naturally fractured reservoirs (NFR) are a challenge for the oil industry due to their importance in hydrocarbon production and the technical complexity they represent. Well productivity in carbonated formations is influenced by fracture systems that govern the fluids flow within reservoirs (Alcantara et al. 2019; Zaremoayedi et al. 2022). The quality of this type of reservoir is defined by two factors: “hydrocarbon storage” and “production capability.” The hydrocarbon storage capacity is defined by the effective porosity and connected pore types located within the confines of a hydrocarbon trap (Peters et al. 2012; Anees et al. 2022). One of the most effective types of porosity is fracture porosity. A slight increase in fracture porosity can cause substantial

✉ Ali Kadkhodaie
Kadkhodaie_ali@tabrizu.ac.ir

¹ Geology Department, Science and Research Branch, Islamic Azad University, Tehran, Iran

² Earth Sciences Department, Faculty of Natural Sciences, University of Tabriz, Tabriz, Iran

³ DWA Energy Limited, Lincoln, UK

⁴ Geology Department, Tehran North Branch, Islamic Azad University, Tehran, Iran

changes in a formation permeability in directions parallel to the fractures. Hence, natural fractures can make significant contributions to permeability and/or porosity, reservoir behavior and field production performance, particularly in carbonate reservoirs (Nelson 2001; Ameen and Hailwood 2008; lai et al. 2017).

It is effective to detect and characterize fracture patterns and their subsurface distributions to better explore and identify potential productive/non-productive zones in oil and gas fields (Jiang et al. 2022; Ashraf et al. 2020; Ullah et al. 2022). Fractures play an important role in many reservoirs in creating possible pathways for hydrocarbon flow and migration by enhancing the overall formation's permeability (Prioul and Jocker 2009; Khoshbakht et al. 2012; Prioul and Jocker 2009; Tokhmchi et al. 2010; Ameen et al. 2012; Khoshbakht et al. 2012; Lyu et al. 2016; Lai et al. 2017; Zahmatkesh et al. 1994; Serra and Serra 2004; Serra 1989; Milad and Slatt 2018; Laongsakul and Dürrast 2010; Saedi et al. 2017). Usually, the behavior of a fractured reservoir is very different from a non-fractured reservoir, due to the higher permeability of fractures compared to the matrix permeability. In this regard, the investigation of fractured reservoirs to quantify their effective porosity and permeability tends to be a lengthy process and more challenging than matrix-controlled reservoirs (Nie et al. 2013; Nelson 2001; Kosari et al. 2017). The heterogeneities of fracture networks often significantly affect the flow performance of fractured reservoirs (Gong and Rossen 2017). If natural fractures are not characterized in early stages of field production, future field development plans can be blurred (Bratton et al. 2006; Alvarez et al. 2020). Unfortunately, natural fractures in oil reservoirs are often ignored or evaluated with oversimplified techniques, leading to the wrong decision being made in exploration and production programs incurring high costs (Voorn et al. 2015). As such a large proportion of known global oil and gas resources is located in naturally fractures reservoirs (NFCRs), the fractures in these reservoirs warrant more detailed and systematic evaluation as fractures are an integral part of petroleum production (Dusseault and Shafiei 2011; Shafiei et al. 2013, 2018). Iran, as one of the largest oil producers in the Middle East and the world, has many fractured carbonate reservoirs. The majority of them are located in the southwest of Iran. It is essential to recognize the fracture patterns and their distributions in these reservoirs, as it paves the way for an exploration, production and development of potential oil and gas fields (Badakhshan et al. 1998; Khoshbakht et al. 2012). This study reports new quantified findings on the impact of *in situ* fractures (open, vuggy, partly filled and filled), bedding planes and stylolites delineated by the Full-bore Formation Micro-Imager (FMI) wellbore log, coupled with information from other petrophysical well logs, on the reservoir quality and potential productivity of the Sarvak Formation. Integration

of FMI, petrophysical logs and core analysis data (porosity and permeability) establish useful relationships between fracture types and densities within the most permeable zones of the Sarvak. The research into systematic tectonic-related fractures provides a better understanding of fracture pattern distributions. Such information can be utilized to improve fracture network modeling. The current study makes efforts to distinguish the relationship between fracture type and fracture density and linking them to interpreted porosity and permeability as an effective tool for improving oil and gas fields development offers. The described indirect fracture analysis method is less expensive than other fracture identification methods and offers the additional advantage of determining the impact of fracture on porosity and reservoir permeability.

Geological setting

The field under study is located in the structural zone referred to as the Abadan Plain, forming part of the Zagros basin (SW Iran). The studied field is situated within the Mesopotamian Foredeep sub-basin that is surrounded by the Arabian Plate and the Dezful Embayment (Saadatinejad and Sarkarinejad 2011). Due to the alluvial overburden, geological knowledge of that sub-basin is limited to wellbore data including drill cuttings, cores, logs and other geophysical data (Assadi et al. 2018). The available data suggest that the Quaternary alluvium along with the subsurface sedimentary layers has been folded in the north–south direction (Motiei 1996, 1993). The Abadan Plain structurally belongs to the Arabian Platform and follows the Arabian-type (N-S) structural trend, which is in contradiction to the typical Zagros-type structural trend (NW–SE) (Shakeri and Parham 2013).

The Dezful Embayment and Abadan Plain (SW Iran, Fig. 1) host a substantial portion of the Iran's oil resources (Abdollahie Fard et al. 2006; Tabatabaei et al. 2015). The Sarvak Formation (Middle Cretaceous), which is the main producing reservoir unit in the studied oilfield, comprises the most prolific carbonate oil reservoir of the Abadan Plain, and the second most important reservoir, in terms of oil and gas production in the entire Zagros Basin (Assadi et al. 2016; Malekzadeh et al. 2020). The Bangestan Group includes the Sarvak and Ilam Formations, which account for approximately 37% of Iran's oil reserves. It is ranked second after the giant Oligo-Miocene Asmari Formation (45%) (Gholami Zadeh 2019; Esrafil-Dizaji and Rahimpour-Bonab 2019).

The Sarvak Formation is a thick carbonate unit deposited in the Neotethys Southern Margin of Zagros Basin (Pakparvar et al. 2017; Bordenave and Hegre 2010; Ezati et al. 2018; Soleimani et al. 2013). In terms of stratigraphy, the Sarvak Formation comprises three types of limestone units reaching a maximum thickness of 821 m. The lower boundary of the

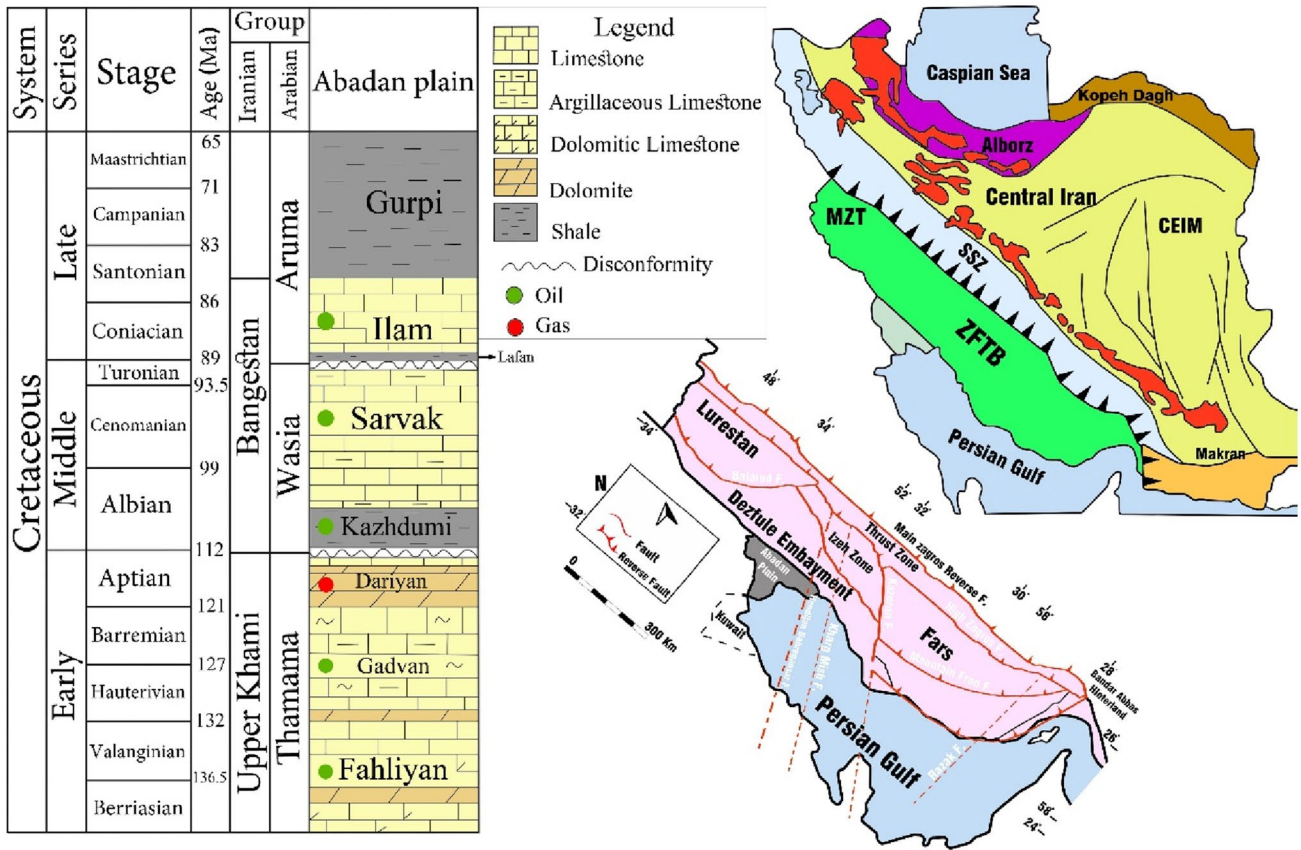


Fig. 1 Zagros structural divisions and stratigraphy column of Abadan Plane

Sarvak Formation overlies the Kazhdumi Formation, while the upper boundary, defined by the Turonian unconformity, varies from place to place. The lower limestone unit of the Sarvak Formation (254.5 m thick) consists of argillaceous micritic limestone with lenticular bedding and thin-layered marl interbeds. The middle Sarvak unit (524.5 m thick) contains massive chalky limestones with iron-rich siliceous carbonates. The top 42 m of the formation includes a massive limestone (unit 3) layer with its uppermost strata consisting of a weathered brecciated ferruginous limestone (Leturmy and Robin 2010). The top of Sarvak Formation is comprised of the Lafan shales (Fig. 1). There are different methods available for detecting the lithology from well-log data. The lithological components of Sarvak Formation were identified in the studied well by applying the density-neutron cross-plot. The density-neutron cross-plot is widely used for distinguishing limestone, dolomite, sandstone, shale and anhydrite (Diana Morton-Thompson 1993). As shown in Fig. 2, the major lithologies present in the studied well are limestone and dolomite. The total porosity of the Sarvak Formation ranges from 2 to 30% and effective porosity ranges from 2 to 27%. The secondary porosity contribution is less than 3%. In this study, the neutron-derived porosity is considered to

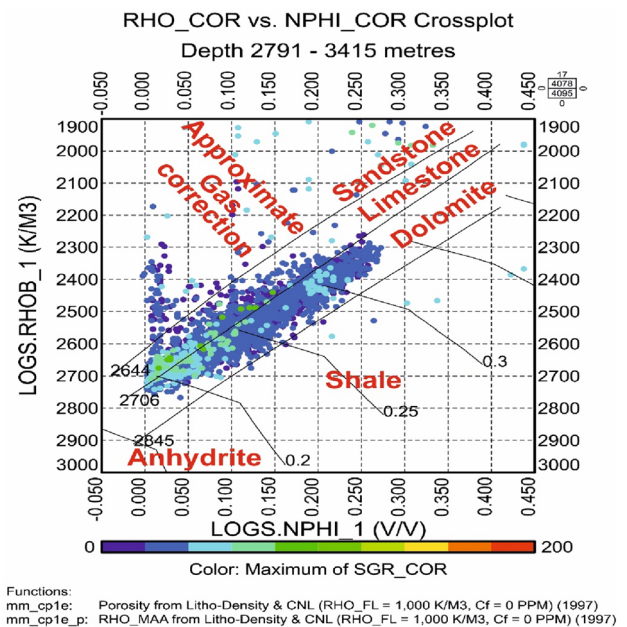


Fig. 2 Corrected neutron-density cross-plot

reflect total porosity, and the sonic-derived porosity is considered to reflect effective porosity. The difference between total and effective porosity is, therefore, considered to be a measure of secondary porosity.

The studied field is associated with a north–south trending anticline. The Sarvak Formation has been completely penetrated by the studied wellbore and image logs, together with a suite of standard petrophysical logs which has been recorded across the formation.

Material and methods

The study is implemented in three stages (Fig. 3): (1) processing and interpretation of image log and petrophysical well logs; (2) classification and data analysis and (3) linking interpreted results to productive/non-productive zones within the Sarvak formation. Initially, raw Full-bore Formation Micro-Imager (FMI) images and petrophysical logs data were corrected for environmental effects. Using the corrected data, sedimentary features such as bedding planes and stylolites, together with tectonic features such as fracture types (continuous open, isolated open, partly filled and filled), were identified and classified. For each identified feature, rose diagrams and density charts were generated to quantify

their characteristics and distributions. Dip analysis software (Dips) was employed to draw contour diagrams of the identified image-log features. DT vs. fracture porosity, NPHI vs. fracture porosity and RHOB vs. fracture porosity cross-plots were generated to investigate the relationship between fractures and petrophysical data. Fracture porosity is obtained using image logs, and matrix porosity is obtained from petrophysical logs. Since fractures are considered as part of effective porosity. Fracture porosity is obtained from the difference between the matrix porosity and the total porosity.

Compared to the Formation Micro-Scanner (FMS) tools, FMI tools are better able to image all parts (360°) of the wellbore wall (Serra 1989), whereas the resistivity image (FMS) represents only about 80% of the borehole coverage in an 8.0-inch diameter borehole (Rider 2002; Brown et al. 2015; Moreau and Joubert 2016; Folkestad et al. 2012). The FMI-oriented image has a vertical resolution of 5 mm (0.2 in.) (Rider 2002; Folkestad et al. 2012; Schlumberger Educational Service 2004; Wilson et al. 2013; Brekke et al. 2017; Lai et al. 2018). To obtain a better model for the relationship between permeability and fracture porosity, image-log-derived fracture density needs to be correlated with other petrophysical log data. Fractures are considered as a planar feature within the formation and after unwrapping the cylindrical borehole, the fractures are seen as a sinusoidal wave on the unwrapped

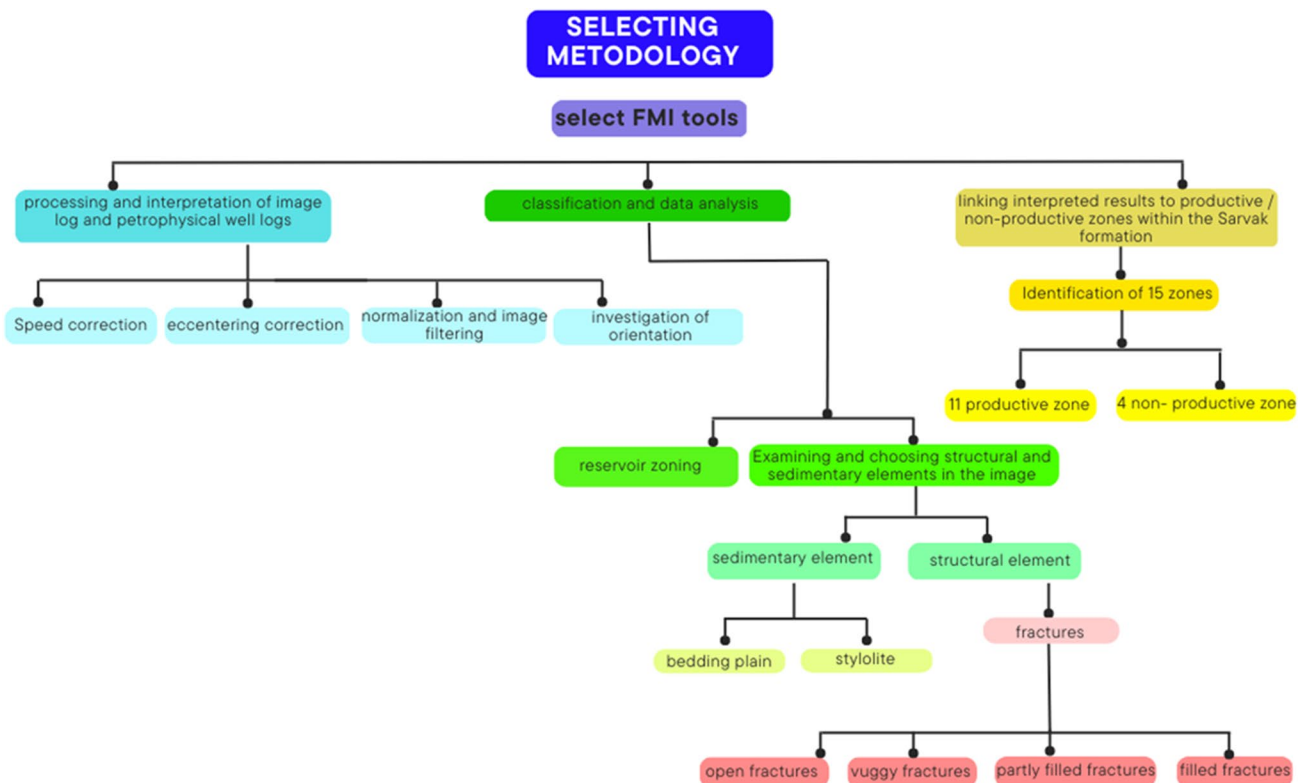


Fig. 3 Flowchart of methodology used in this study for fracture characterization

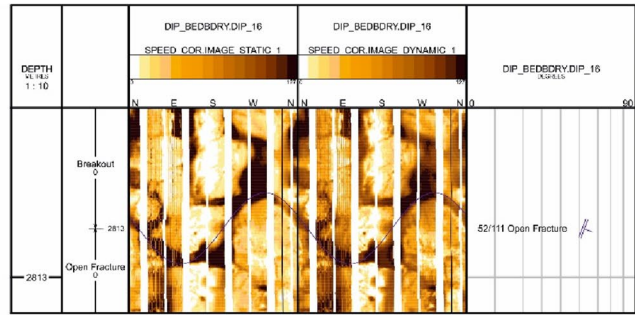
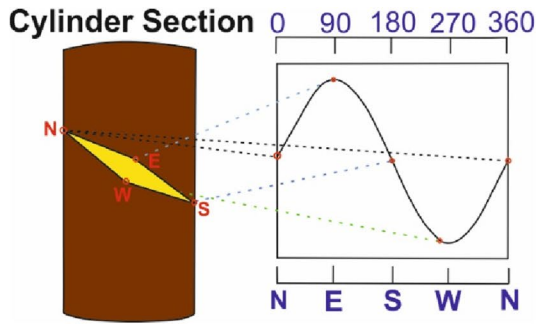


Fig. 4 Sketch showing the appearance of a fracture intersecting a wellbore at an inclined angle, and how it displays on an unwrapped image log as a sinusoidal pattern

image logs (Fig. 4). Relatively high and sudden changes in electrical resistance are features of fractures that can be differentiated by their changing color and with trends that extend through substantial sections of the FMI images. Fractures may be filled with a variety of materials, each of which is associated with a different resistivity. Resistivity values recorded by the image log are less than the background rock when the fractures are filled with conductive materials.

Results

According to the drilling and petrophysical data, Sarvak Formation in the studied well includes 15 zones, 11 of which are recognized as oil zones (Fig. 5). Natural fractures identified in this study were divided into four categories including open fractures, vuggy fractures, partly-filled fractures and filled fractures. Open fractures are the most widespread types of fractures in the well (Fig. 6). Usually, the presence of open fractures controls the permeability in the carbonate reservoirs (Ngwenya et al. 2003; Boro et al. 2014; Li et al. 2018; Shafiei et al. 2018; Bagheri and Falahat 2022). In other words, one of the most important factors controlling the fluid transmissibility in the reservoir is the presence of natural open fractures. Accordingly, petroleum engineers can pay more attention to open and vuggy fractures compared to the other types of fractures, as they are more likely to be associated with the fluid flow and productivity. Each fracture set can be investigated in terms of the orientation of individual features (Figs. 6 and 7). In addition, the density of occurrence can be compared for each feature versus depth to determine the frequency distribution of each type of feature and relationships between those frequency distributions.

Natural fractures interpretation

A total of 117 natural fractures were detected that could be divided into four categories including open fractures,

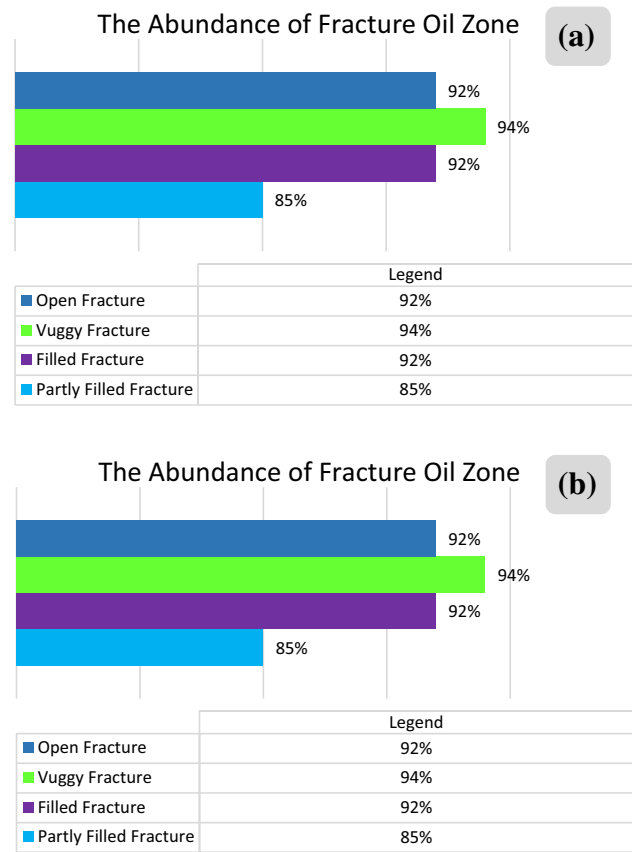


Fig. 5 Abundance of fractures: **A** in Sarvak Formation of studied well (2791–3415 m) and **B** in oil-producing zone of studied well (3791–3000 m)

vuggy fractures, partly-filled fractures and filled fractures. The number of open fractures is 55, which are divided into three main sets with average dips and dip azimuths about 43°/336°, 47°/92° and 45°/228°, respectively. The number of vuggy fractures is 35, and they consist of two main categories with an average dip and dip azimuth about 44°/253° and 42°/045°, respectively. It seems that partly-filled and filled

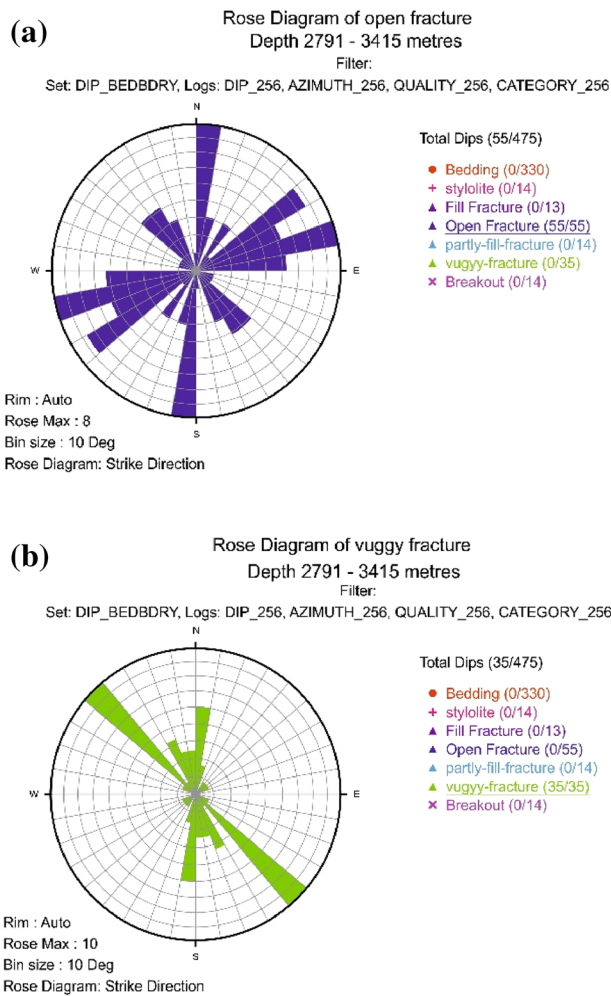


Fig. 6 Rose diagram of open fractures (a) and vuggy fractures (b)

fractures have the same origin because their dispersions are centered at about the same depth. Also, these two features have the same orientation according to contour diagrams. There are 14 partly-filled fractures, with an average dip and dip azimuth of about $46^\circ/350^\circ$. The number of filled fractures is 13, with an average dip and dip azimuth of about $42^\circ/003^\circ$ (Figs. 6, 7 and 8). The results show that as the magnitude of fracture porosity increases, the DT and NPHI log values increase but density readings decrease.

Bedding plane control on fracture density

According to the drilling and petrophysical data, the studied well has 11 oil-producing zones; the highest numbers of fractures were found in these zones. The fracture density log (Fig. 8) shows that the highest fracture density is in the upper part of the Sarvak Formation. The maximum density is from the depth of 2791 to 3000. According to the

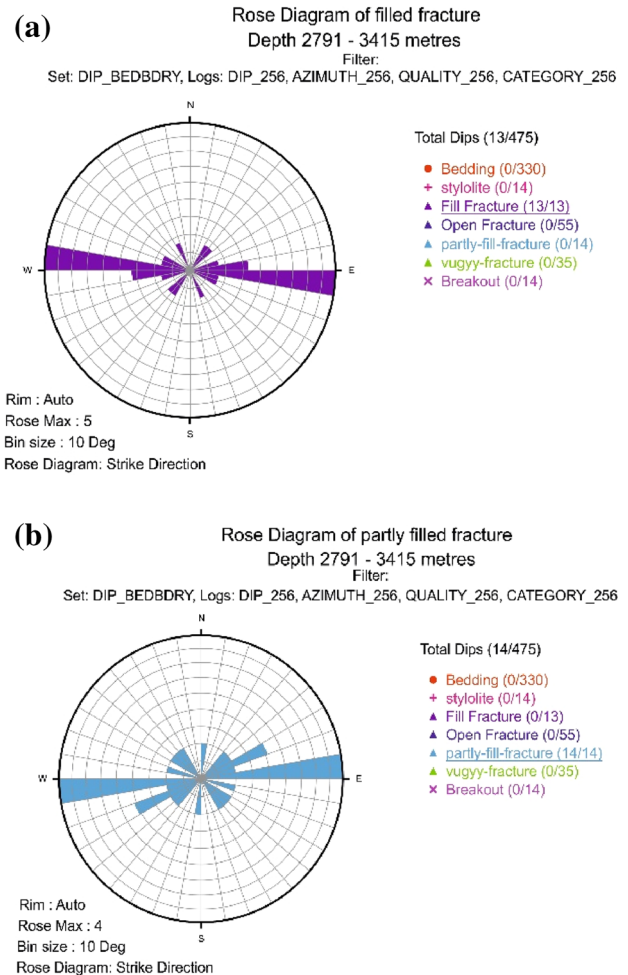
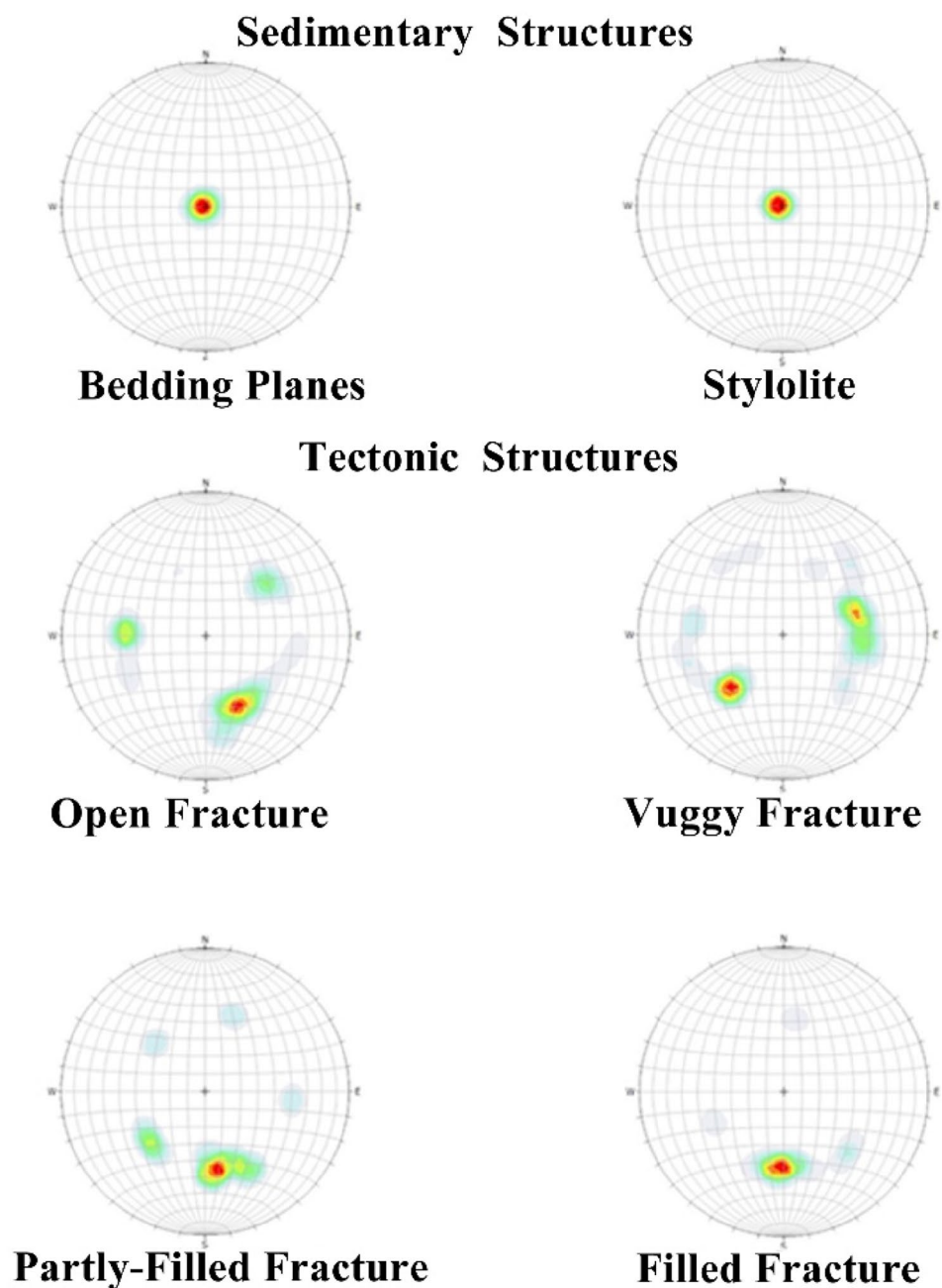


Fig. 7 Rose diagram of filled fractures (a) and partly-filled fractures (b)

frequency diagram, the upper parts of well display more massive layering, while thinner layers characterize the lower parts of the Sarvak Formation (Fig. 9).

In the studied well, 384 bedding planes were identified according to variations in color and/or lithology. The average dip of the bedding planes is 2° (i.e., almost horizontal), and the mean azimuth is 81° . Comparison made between fracture density and bedding revealed that fracture density in thick-bedded intervals is greater than in the thin-bedded zones (Fig. 9). A total of 14 stylolites were identified in the studied well. Stylolites are seen in image logs in the form of conductive, often flat or wave-like lines with near-vertical, short components oscillating unevenly through the formation. The average dip of stylolites in the well is 2 degrees (i.e., almost horizontal), and the mean azimuth is 89° . Stylolites in this well are primarily parallel with the bedding planes, suggesting that they have a sedimentary origin. They are common in cemented and compact carbonate intervals around the world (Fig. 10).

Fig. 8 Lower-hemisphere pole projection for all fractures, stylolites and bedding planes

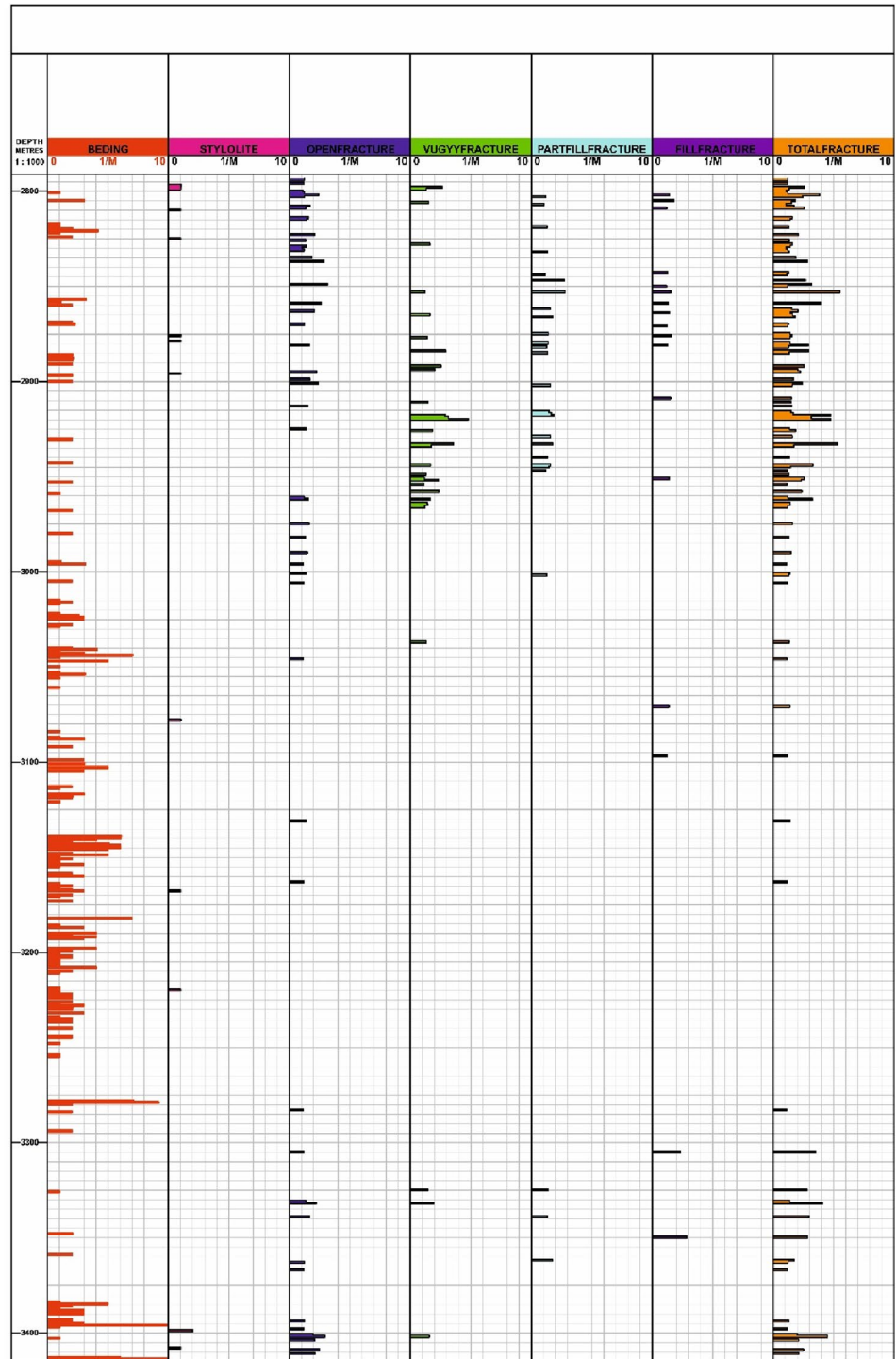


Fracture density relationships with permeability and production flow rates

According to the fracture density diagram, the Sarvak reservoir in the studied well can be divided into two parts: an upper part with high fracture density between 2791 and 3070 m and a lower part with very low fracture frequency between 3070 and 3415 m. The Sarvak Formation has thick, massive layers in the upper part and thin layering in the lower part. By constructing fracture density and porosity diagrams and matching them with the reservoir permeability logs (Fig. 11), it is apparent that in the upper parts of the

well, the fracture density is high. This high fracture density contributes substantial fracture porosity to certain zones of in the upper part of the Sarvak Formation and increases the permeability in those zones. Of the 15 zones in the studied well, 11 of them can be considered as potentially productive zones. Some 93% of the continuous open fracture, and isolated open fractures are located in these 11 zones. These 11 zones extend between depths of 2791 and 3070 m. In this study, two types of continuous open fracture and isolated open fracture are considered as fractures with a positive effect on porosity and permeability in the Sarvak reservoir. Figure 12 shows the cross-plot of fracture density

Fig. 9 Density (fractures per 1/M) logs of bedding planes (track 2), stylolites (track 3), open fractures (track 4), vuggy fractures (track 5), partly-filled fractures (track 6), filled fractures (track 7) and total fractures (track 8)



versus permeability. The permeability clearly increases with increasing frequency of fractures (Fig. 13).

In the zones where the fracture density is greatest (Fig. 11), it can be seen that fracture porosity contributes a much larger portion to the total porosity. By considering the permeability log, calculated porosity and frequency of fractures together, it is generally apparent that fracture porosity correlates positively with permeability. The results of

production tests show that for the depth interval 2791–3070, oil production rate was 1996 bbl/d, and the gas production was 0.6 mmmcf/d. Figures 14, 15, 16, 17 and 18 display composite logs related to specific zones within the Sarvak Formation of the studied well.

In the lower part of the studied well (3070–3415), there is no oil production. This could be an indication of that depth interval being outside of structural closure, or that

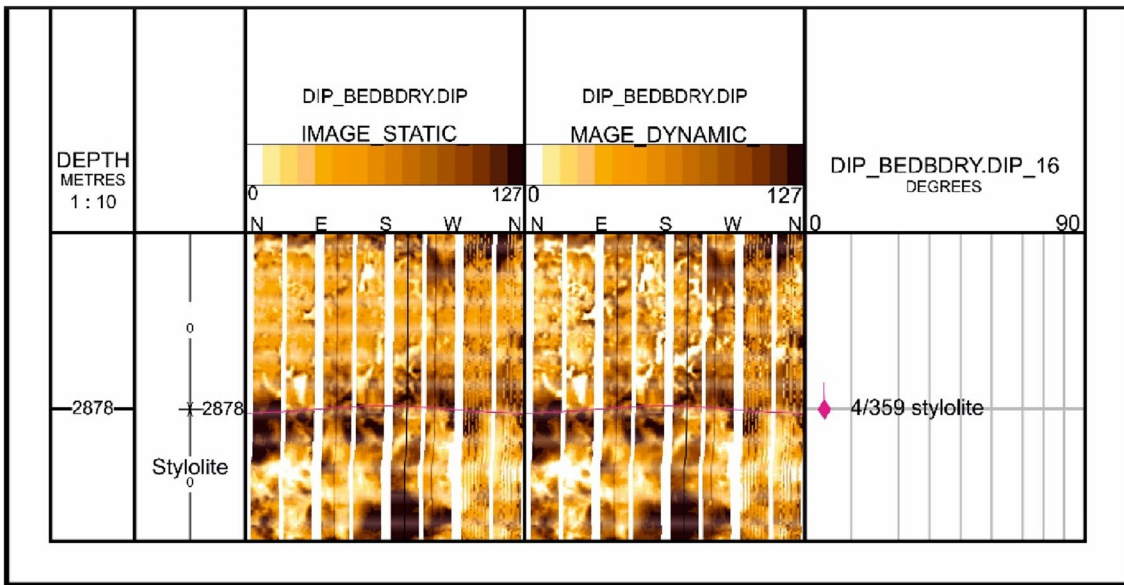


Fig. 10 An image-log example of a stylolite in the studied well (2878 m)

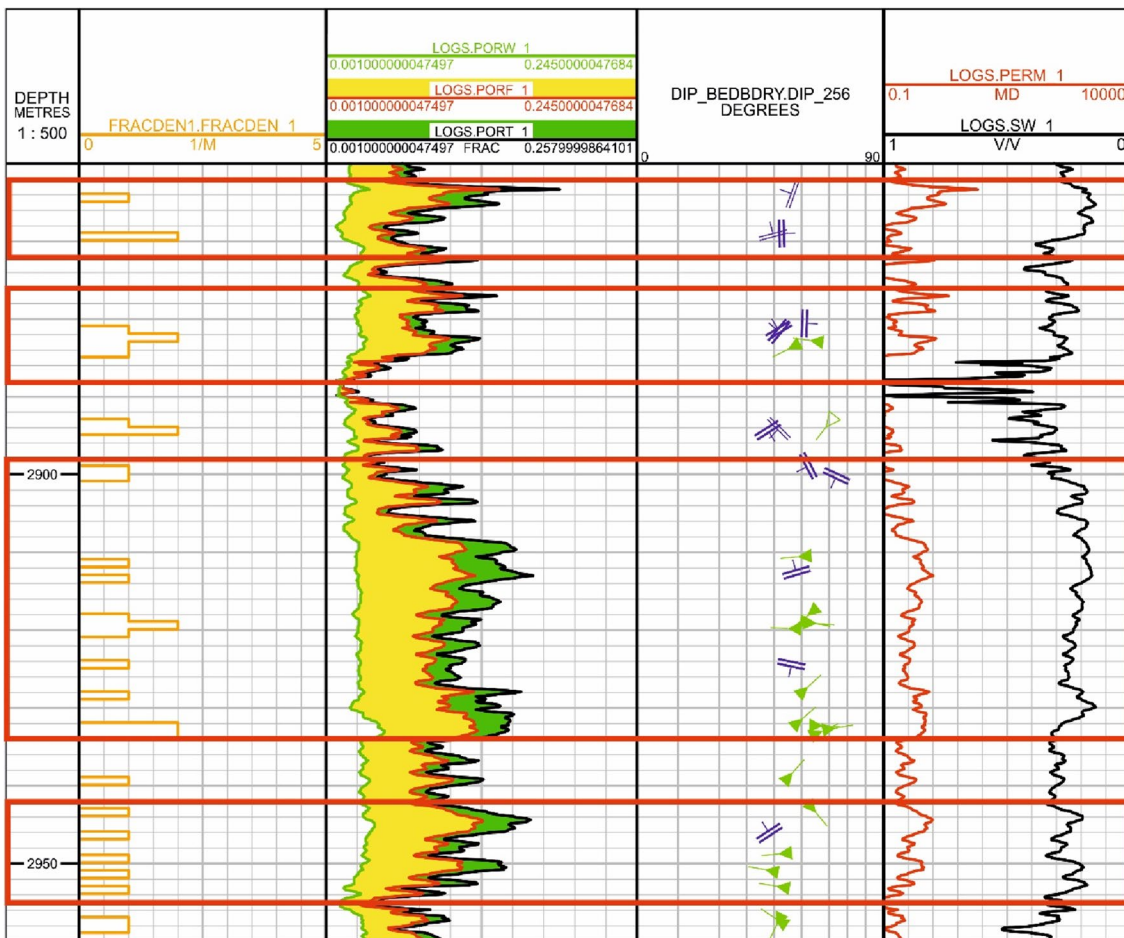


Fig. 11 Permeability variations across the fractured zones

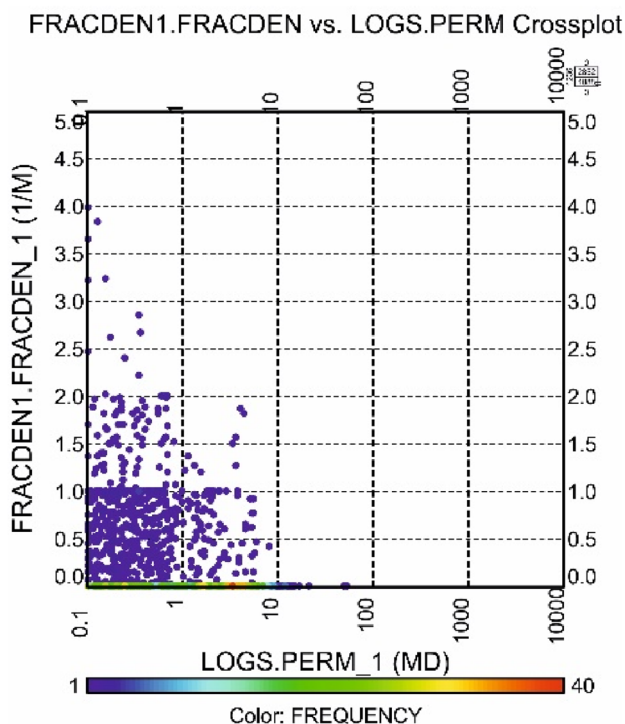


Fig. 12 Cross-plot of fracture density versus permeability

not enough volume of charged hydrocarbons was available to fill the structural trap resulting in high water saturation, or the absence of sufficient fractures in this lower reservoir zone. The latter factor is likely to result in ineffective porosity in that lower portion of the reservoir. In fact, that lower zone produced between 2.4 and 84 bbl/d of salty water (300,000 ppm salinity). The water saturation in the lower Sarvak reservoir zone is high reaching 100% in places (Fig. 18). Despite sufficient porosity and permeability existing to sustain production from the depth interval 3070 to 3415 m, that zone was only able to produce modest amount of water. Consequently, it is more likely that this lower reservoir zone is both deprived of sufficient hydrocarbon charge and its low density of open fractures limits its flow potential.

Discussion

Fractures play a vital role in production and migration of oil in the majority of Iranian hydrocarbon reservoirs, particularly those with carbonate lithologies. Therefore, detailed fracture evaluation and detection is essential for maximizing production from fractured intervals. Fractures in carbonate reservoirs are important due to their high influence on reservoir rock properties, particularly porosity and permeability (Nelson 2001; Rajabi et al. 2010; Aghli et al. 2016; Zaree et al. 2015).

There are some direct and indirect methods that can be used for fracture characterization in carbonate reservoirs. For this purpose, geoscientists and petroleum engineers have used various data such as geophysical data, log data, drilling cores and surface outcrops to describe the fractures and their characteristics (Fang et al. 2017; Dong et al. 2020; Li et al. 2018; Bagheri and Falahat 2022; Ashraf et al. 2021; Anees et al. 2022). However, all of these methods encounter serious constraints and limitations. For example, seismic can only show large-scale fractures and faults, and also, cores have vital limitations such as low recovery factor in fractured zones, orientation issues and the high cost of coring. Using petrophysical logs and FMI (or other image log) data provides a useful and rapid method to determine fractures present in a wellbore (Aghli et al. 2016). Compared with other types of borehole image-log tools, the FMI tool is capable of covering a substantial part of borehole wall (Serra 1989), and the resistivity image represents about 80% of the borehole walls, in an 8.0-inch diameter borehole (Moreau and Joubert 2016; Folkestad et al. 2012). The oriented FMI image has a vertical resolution capable of recording details as small as 5 mm (0.2 inch) (Folkestad et al. 2012; Schlumberger Educational Services 2004; Wilson, et al. 2013). The high-definition FMI (FMI-HD) tool is an improved imaging tool (Schlumberger) (Lai et al. 2018). For these reasons, the FMI data have been selected for fracture analysis in the studied wellbore.

Finding a quick method for identification of fractured zones using petrophysical logs and FMI data, which are available in most wells is a vitally important challenge in production and exploration of oil and gas reservoir. Among many of the presented methods, acoustic logs have especial and practical applications in the carbonate reservoirs, because they show primarily matrix porosity, and they are affected by fractures. Acoustic waves, including compressional, shear and Stoneley waves, are sensitive to reservoir properties such as fractures and permeability. Tokhmchi et al. (2010) proposed a method for fracture density estimation in the fractured zones using the energy responses of petrophysical logs. They calculated the energy of the petrophysical logs in the fractured zones, and then, linear and nonlinear regressions were applied to determine fracture density. More generally, results have shown that there is a strong correlation between the energy of caliper, sonic (DT), density (RHOB) and photoelectric absorption factor (PEF) logs with fracture density in many wells (Taherdangkoo and Abdideh 2016; Yang et al. 2017; Azizi and Reza 2021).

The novel method developed in this study to distinguish fracture type and fracture density, and link that information to log-interpreted porosity and permeability data, offers substantial potential to improve oil and gas field development. The indirect fracture analysis method described is less expensive than other methods of fracture

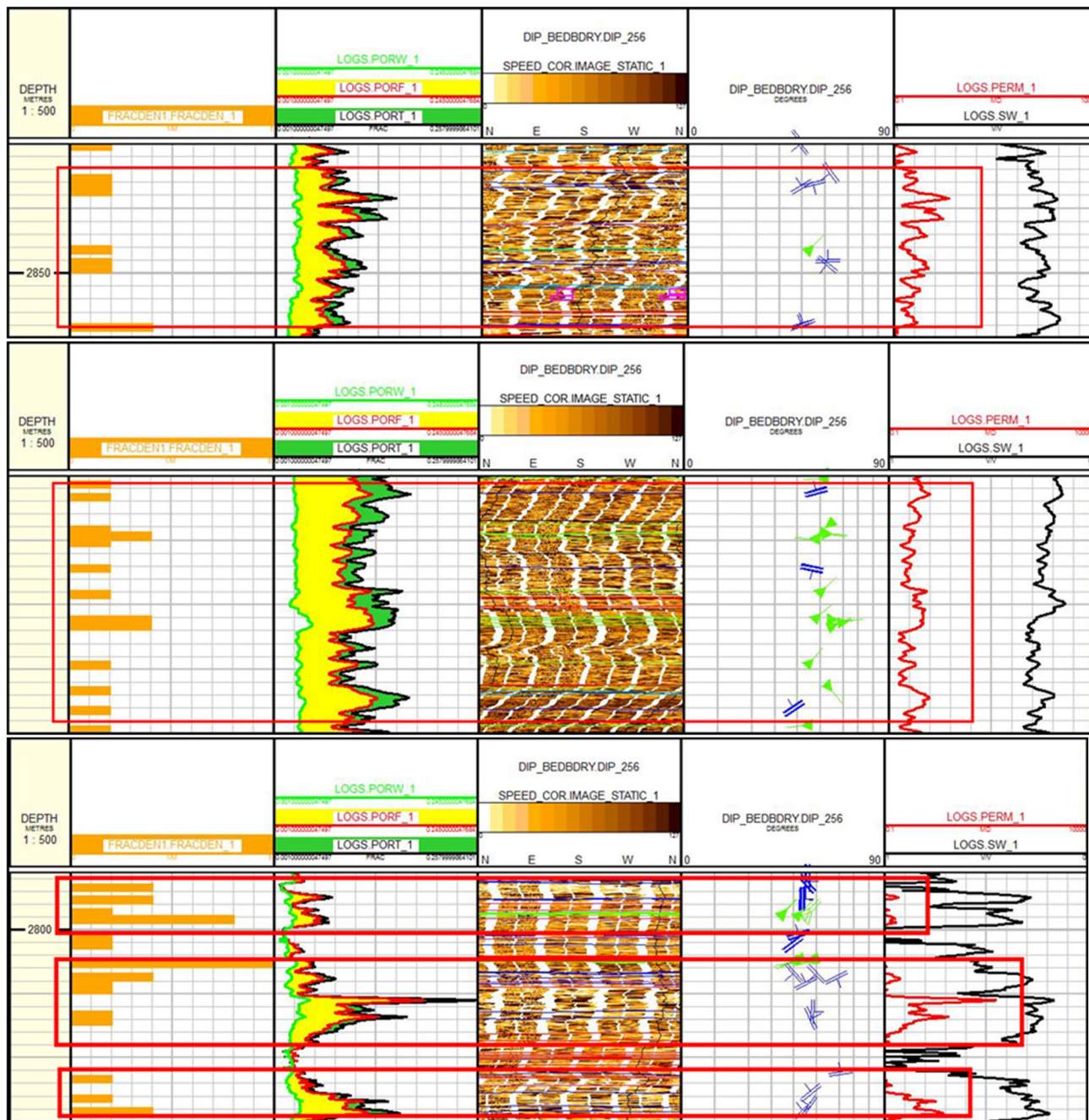


Fig. 13 Permeability variation with fracture density in fractured zones

identification and provides the additional benefit of determining fracture porosity and its effects on reservoir permeability. The potential exists to correlate reservoir zones with specific fracture types and densities from one well to another across a reservoir. This could facilitate mapping prospective zones within a reservoir with volumes that do not necessarily lie within specific bedding planes or stratigraphically-defined intervals. In cases where other information is available such as core information (with

high recovery) and/or specialist petrophysical logs, fracture type using the proposed method could be usefully correlated with other rock properties. This method can be extremely beneficial in assisting with field development decisions by providing highly accurate and detailed fracture analysis at low cost. In particular, it can help to design specific trajectories for planned deviated production wells, ensuring that they encounter the most productive fractured reservoir zones at the optimum orientation.

Fig. 14 Composite well log for production zones within depth interval 2790–2825 m

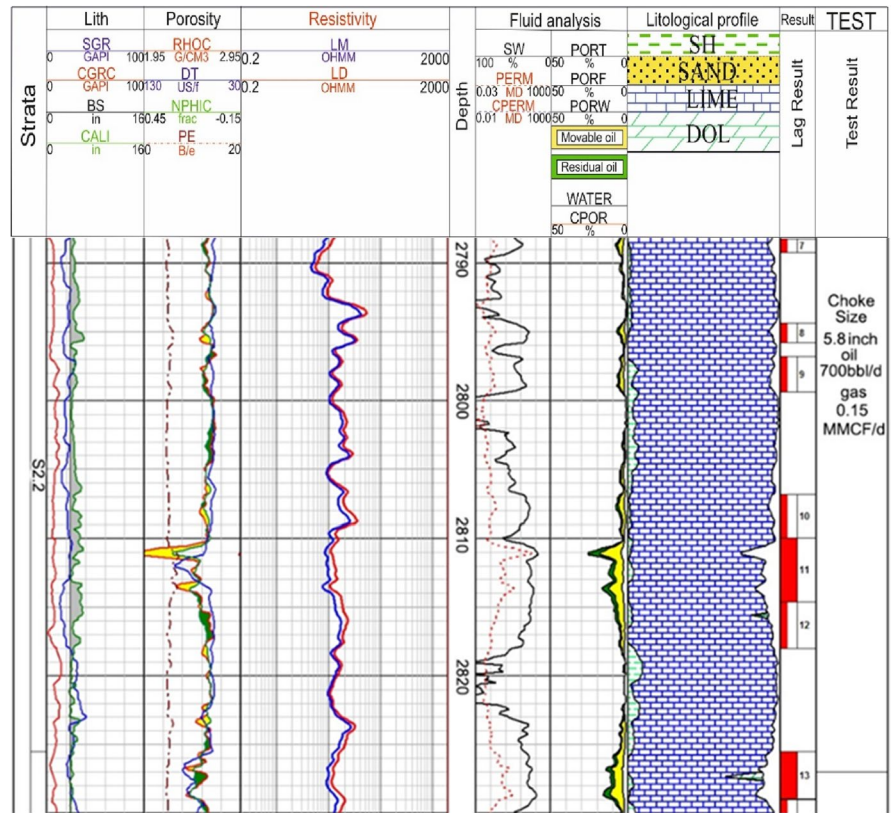


Fig. 15 Composite well log for production zones within depth interval 2830–2860 m

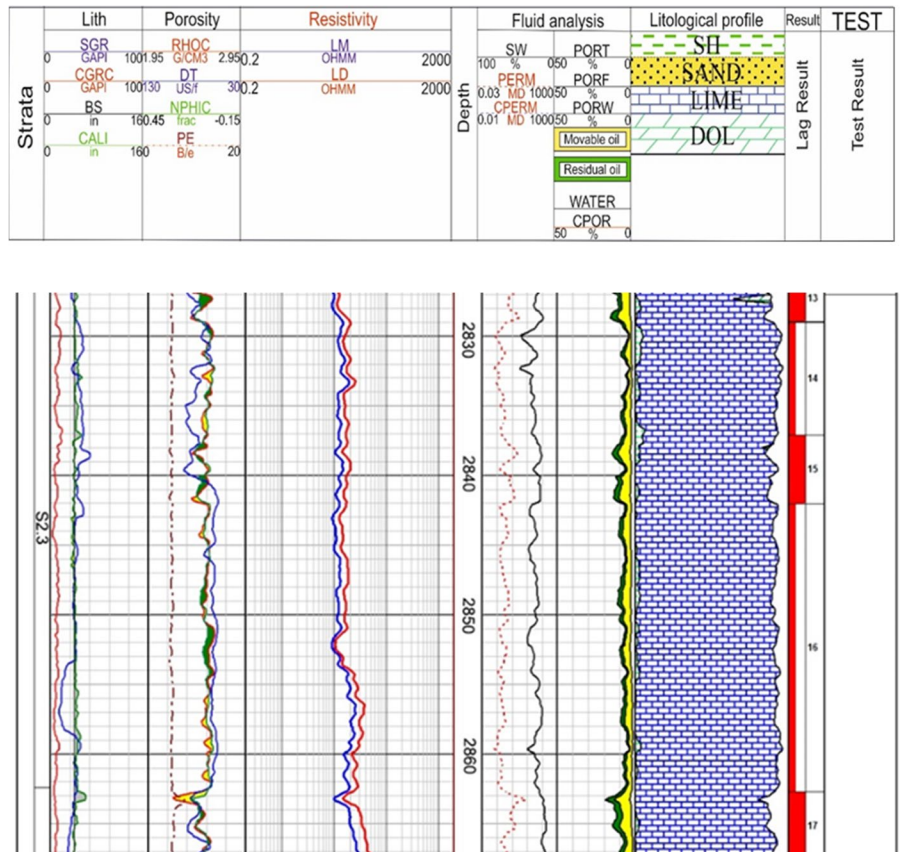


Fig. 16 Composite well log for production zones within depth interval 2870–2900 m

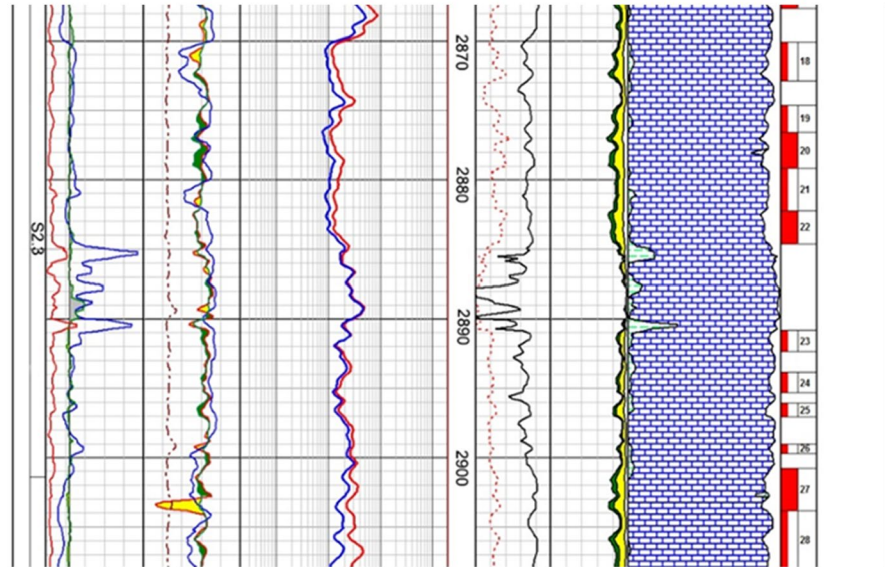
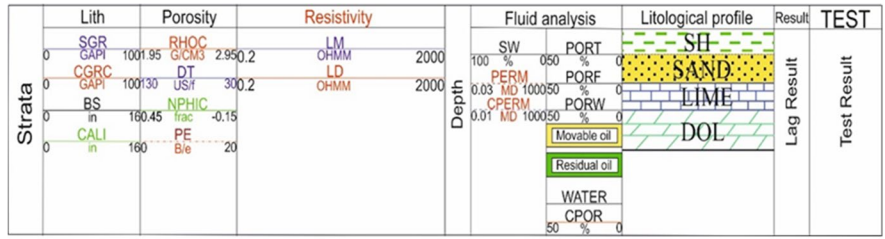


Fig. 17 Composite well log for production zones within depth interval 2910–2950 m

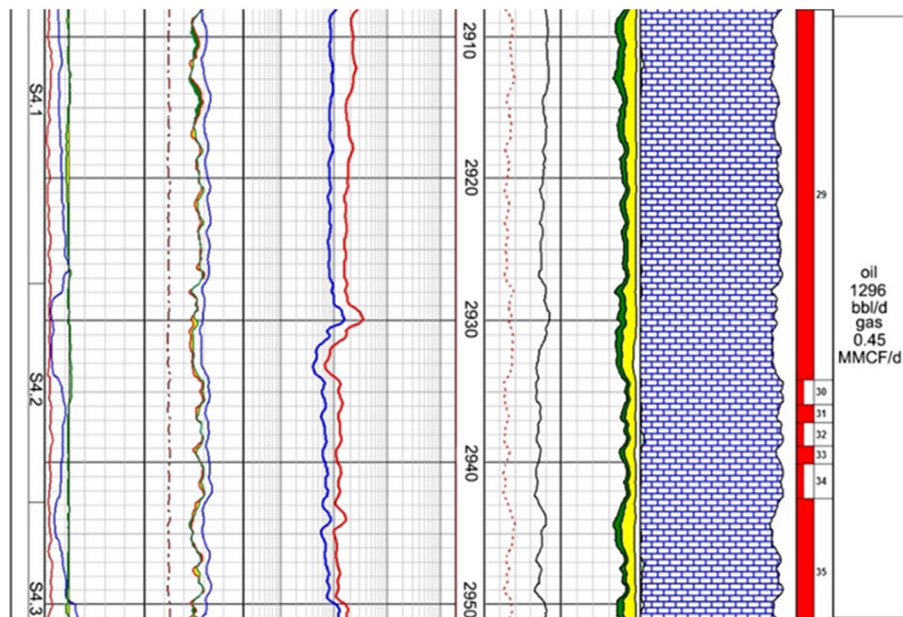
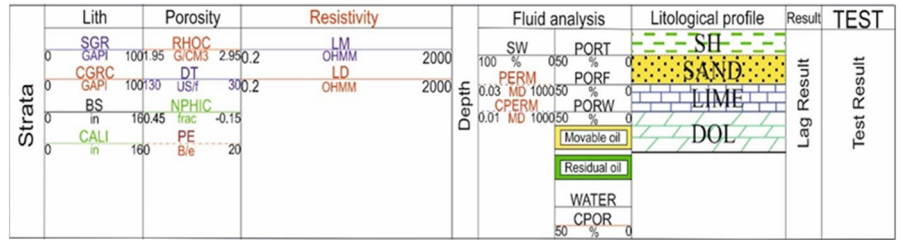
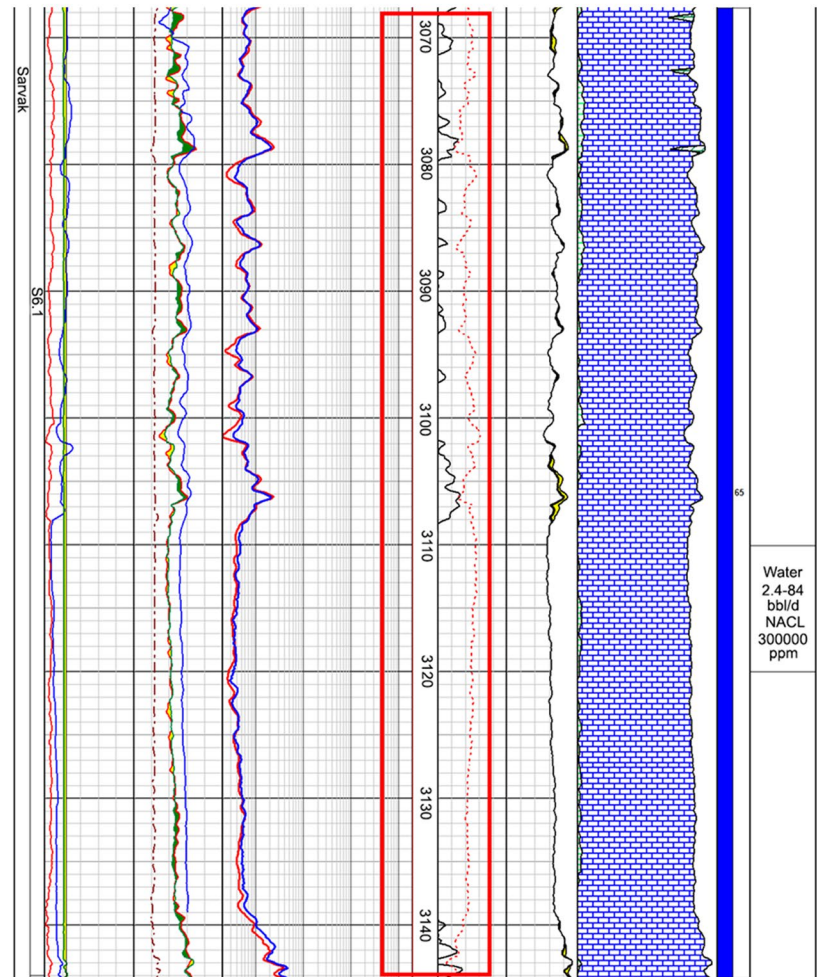
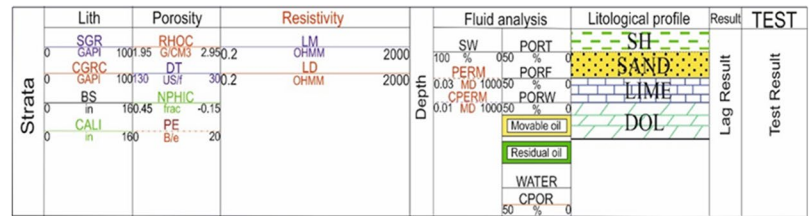


Fig. 18 Composite well log for the non-productive zone of the studied well which flowed saline water from depth interval 3070–3140 m



Conclusion

Considering the results obtained from image logs of this study, the followings are concluded.

- Bedding planes are determined to be oriented predominantly in N–S directions with an average dip and dip azimuth about 2 degrees and 79 degrees, respectively. A total of 117 natural fractures were detected that could be divided into four categories including open fractures, vuggy fractures, partly-filled fractures and filled fractures. A total of 55 open fractures were detected,

and these are divided into three main sets. Average dip and dip azimuth of the three sets of open fracture are about $43^\circ/336^\circ$, $47^\circ/92^\circ$ and $45^\circ/228^\circ$, respectively. The number of vuggy fractures detected was 35. This type of fracture consists of two main categories with average dip and dip azimuth of about $44^\circ/253^\circ$ and $42^\circ/045^\circ$, respectively. It seems that these two categories of vuggy fractures have the same origin as their dispersion is about the same depth. Also, these two sets have the same orientations according to contour diagrams. The number of partly-filled fractures detected was 14, with an average dip and dip azimuth about $46^\circ/350^\circ$, respectively. The

number of filled fractures detected was 13, with an average dip and dip azimuth of about $42^{\circ}/003^{\circ}$.

- The porosity volume experiences some changes throughout the Sarvak Formation. Total porosity changes were measured in the formation from 2 to 30%. Matrix porosity varied from 2 to 27%, indicating that secondary (fracture) porosity has less than 3% contribution to total porosity. Although the amount of fracture porosity is very low, it seems to have contributed substantially to permeability in the well sections where the density of open and vuggy fractures is high.
- Change in the permeability diagram combined with change in fracture density in formation zones, where permeability has increased, is likely to be caused by the density and type of the fractures present.
- By comparing the petrophysical and density diagrams, we find that the upper part of the Sarvak reservoir (2791–3000 m) has good reservoir potential for exploitation and enhanced oil recovery (EOR).
- Matrix porosity in this section shows a substantial increase, suggesting that it has good potential to become a productive oil and gas reservoir.
- Future development of the studied field would benefit from drilling vertical wells in the upper Sarvak Formation where open fractures exist. Most of the fractures which were detected in the studied well were open.
- Typically, in the studied well, high permeability is located in specific zones of the Sarvak Formation corresponding to those zones displaying a high density of open fractures. Four high-density fracture zones were identified in the Sarvak Formation based on the integrated image log and other available petrophysical data.

Funding This research does not received any funding.

Declarations

Conflict of interest The authors declare that they have no known competing financial interests or personal relationships that could have appeared to influence the work reported in this paper.

Ethical approval This material is the authors' own original work, which has not been previously published elsewhere. The paper is not currently being considered for publication elsewhere. The paper reflects the authors' own research and analysis in a truthful and complete manner. The publication of this manuscript does not engage in or participate in any form of malicious harm to another person or animal.

Open Access This article is licensed under a Creative Commons Attribution 4.0 International License, which permits use, sharing, adaptation, distribution and reproduction in any medium or format, as long as you give appropriate credit to the original author(s) and the source, provide a link to the Creative Commons licence, and indicate if changes

were made. The images or other third party material in this article are included in the article's Creative Commons licence, unless indicated otherwise in a credit line to the material. If material is not included in the article's Creative Commons licence and your intended use is not permitted by statutory regulation or exceeds the permitted use, you will need to obtain permission directly from the copyright holder. To view a copy of this licence, visit <http://creativecommons.org/licenses/by/4.0/>.

References

- Abdollahie Fard I, Braathen A, Mokhtari M, Alavi SA (2006) Interaction of the Zagros fold-thrust belt and the Arabian-type, deep-seated folds in the Abadan plain and the Dezful Embayment, SW Iranian. *Pet Geosci* 12:347–362. <https://doi.org/10.1144/1354-079305-706>
- Aghli G, Soleimani B, Moussavi-Harami R, Mohammadian R (2016) Fractured zones detection using conventional petrophysical logs by differentiation method and its correlation with image logs. *J Petrol Sci Eng* 142:152–162
- Alcantara R, Santiago LH, Fuentes G, Garcia H, Romero P, López P, Angulo B, Martínez MI (2019) A dynamic characterization approach for a complex naturally fractured reservoir. In: International petroleum technology conference, OnePetro
- Alvarez LL, Beserra L, Guimarães L, Maciel B, Manzoli O (2020) Modeling of near-wellbore permeability reduction due to depletion of a naturally fractured reservoir. In: 54th US rock mechanics/geomechanics symposium. <https://onepetro.org/ARMAU/SRMS/proceedingsabstract/ARMA20/All-ARMA20/ARMA-2020-1659/448813>.
- Ameen MS, Hailwood EA (2008) A new technology for the characterization of microfractured reservoirs (test case: Unayzah reservoir, Wudayhi field, Saudi Arabia). *AAPG Bull* 92(1):31–52. <https://doi.org/10.1306/08200706090>
- Ameen MS, MacPherson K, Al-Marhoon MI, Rahim Z (2012) Diverse fracture properties and their impact on performance in conventional and tight-gas reservoirs, Saudi Arabia: the Unayzah, South Haradh case study. *Unayzah conventional and tight-gas fractures*. *AAPG Bull* 96(3):459–492. <https://doi.org/10.1306/06011110148>
- Anees A, Zhang H, Ashraf U, Wang R, Liu K, Mangi HN, Jiang R, Zhang X, Liu Q, Tan S, Shi W (2022) Identification of favorable zones of gas accumulation via fault distribution and sedimentary facies: insights from Hangjinqi area Northern Ordos Basin. *Front Earth Sci* 9:822670
- Ashraf U, Zhang H, Anees A, Nasir Mangi H, Ali M, Ullah Z, Zhang X (2020) Application of unconventional seismic attributes and unsupervised machine learning for the identification of fault and fracture network. *Appl Sci* 10(11):3864
- Ashraf U, Zhang H, Anees A, Mangi HN, Ali M, Zhang X, Imraz M, Abbasi SS, Abbas A, Ullah Z, Ullah J (2021) A core logging, machine learning and geostatistical modeling interactive approach for subsurface imaging of lenticular geobodies in a clastic depositional system SE Pakistan. *Nat Resour Res* 30(3):2807–2830
- Assadi A, Honarmand J, Moallemi SA, Abdollahie-Fard I (2016) Depositional environments and sequence stratigraphy of the Sarvak formation in an oil field in the Abadan plain SW Iran. *Facies* 62:26. <https://doi.org/10.1007/s10347-016-0477-5>
- Assadi A, Honarmand J, Moallemi SA, Abdollahie-Fard I (2018) An integrated approach for identification and characterization of palaeo-exposure surfaces in the upper Sarvak formation of Abadan plain, SW Iran. *J Afr Earth Sci* 145:32–48. <https://doi.org/10.1016/j.jafrearsci.2018.05.002>

- Azizi H, Reza H (2021) Applied machine learning methods for detecting fractured zones by using petrophysical logs. *Intell Control Autom* 12(2):44–64
- Badakhshan A, Golshan H, Musavi-Nezhad HR, Sobbi FA (1998) The impact of gas injection on the oil recovery of a giant naturally fractured carbonate reservoir. *J Can Pet Technol*. <https://doi.org/10.2118/98-12-01>
- Bagheri H, Falahat R (2022) Fracture permeability estimation utilizing conventional well logs and flow zone indicator. *Pet Res* 7(3):357–365
- Bordenave ML, Hegre JA (2010) Current distribution of oil and gas fields in the Zagros Fold Belt of Iran and contiguous offshore as the result of the petroleum systems. *Geol Soc Lond Spec Publ* 330(1):291. <https://doi.org/10.1144/SP330.14>
- Bratton T, Canh DV, Que N, Van Duc NV, Gillespie P, Hunt D, Li B, Marcinew R, Ray S, Montaron B, Nelson R (2006) The nature of naturally fractured reservoirs. *Oilfield Rev* 18(2):4–23
- Brekke H, MacEachern JA, Roenitz T, Dashtgard SE (2017) The use of micro resistivity image logs for facies interpretations: an example in point-bar deposits of the McMurray formation Alberta Canada. *AAPG Bull* 101(5):655–682
- Brown J, Davis B, Gawankar K, Kumar A, Li B, Miller CK, Laronga R, Schlicht P (2015) Imaging: getting the picture downhole. *Oilfield Rev* 27(2):4–21
- Morton-Thompson D, Woods AM (Eds) (1993) Development geology reference manual: AAPG methods in exploration series. AAPG, Tulsa
- Dong S, Zeng L, Lyu W, Xia D, Liu G, Wu Y, Du X (2020) Fracture identification and evaluation using conventional logs in tight sandstones: a case study in the Ordos Basin China. *Energy Geosci* 1(3–4):115–123
- Dou Q, Sun Y, Sullivan C (2011) Rock-physics-based carbonate pore type characterization and reservoir permeability heterogeneity evaluation, upper san Andres reservoir, Permian Basin, west Texas. *J Appl Geophys* 74(1):8–18
- Dusseault MB, Shafiei A (2011) Oil sands. *Ullmann's encyclopedia of chemical engineering*. Wiley, Hoboken, pp 52
- Esfrafil-Dizaji B, Rahimpour-Bonab H (2019) Carbonate reservoir rocks at giant oil and gas fields in SW Iran and the adjacent offshore: a review of stratigraphic occurrence and poro-perm characteristics. *J Pet Geol* 42(4):343–370
- Esfrafil-Dizaji B, Rahimpour-Bonab H, Mehrabi H, Afshin S, Kiani-Harchegani F, Shahverdi N (2015) Characterization of rudist-dominated units as potential reservoirs in the middle Cretaceous Sarvak formation SW Iran. *Facies* 61(3):1–25
- Ezati M, Azizzadeh M, Riahi MA, Fattahpour V, Honarmand J (2018) Characterization of microfractures in carbonate Sarvak reservoir, using petrophysical and geological data, SW Iran. *J Petrol Sci Eng* 170:675–695
- Fang J, Zhou F, Tang Z (2017) Discrete fracture network modelling in a naturally fractured carbonate reservoir in the Jingbei oilfield China. *Energies* 10(2):183
- Folkestad A, Veselovsky Z, Roberts P (2012) Utilising borehole image logs to interpret delta to estuarine system: a case study of the subsurface lower jurassic cook formation in the Norwegian northern North Sea. *Mar Pet Geol* 29(1):255–275
- Gong J, Rossen WR (2017) Modeling flow in naturally fractured reservoirs: effect of fracture aperture distribution on dominant sub-network for flow. *Pet Sci* 14(1):138–154
- Jiang R, Zhao L, Xu A, Ashraf U, Yin J, Song H, Su N, Du B, Anees A (2022) Sweet spots prediction through fracture genesis using multi-scale geological and geophysical data in the karst reservoirs of Cambrian Longwangmiao carbonate formation, Moxi-Gaoshiti area in Sichuan Basin, South China. *J Petrol Explor Prod Technol* 12(5):1313–1328
- Khoshbakht F, Azizzadeh M, Memarian H, Nourozi GH, Moallemi SA (2012a) Comparison of electrical image log with core in a fractured carbonate reservoir. *J Pet Sci Eng* 86:289–296
- Kosari E, Kadkhodaie A, Bahroudi A, Chehrizi A, Talebian M (2017) An integrated approach to study the impact of fractures distribution on the Ilam-Sarvak carbonate reservoirs: a case study from the Strait of Hormuz, the Persian Gulf. *J Petrol Sci Eng* 152:104–115
- Lai J, Wang G, Fan Z, Wang Z, Chen J, Zhou Z, Wang S, Xiao C (2017) Fracture detection in oil-based drilling mud using a combination of borehole image and sonic logs. *Mar Pet Geol* 84:195–214
- Lai J, Wang G, Wang S, Cao J, Li M, Pang X, Han C, Fan X, Yang L, He Z, Qin Z (2018) A review on the applications of image logs in structural analysis and sedimentary characterization. *Mar Pet Geol* 95:139–166. <https://doi.org/10.1016/j.marpetgeo.2018.04.020>
- Laongsakul P, Dürrast H (2010) Characterization of reservoir fractures using conventional geophysical logging (thesis MSc Prince of Songkla University Faculty of Science (Geophysics)). <https://kb.psu.ac.th/psukb/handle/2010/8873>
- Lee H, Lee SG, Doyle PS (2015) Photopatterned oil-reservoir micro-models with tailored wetting properties. *Lab Chip* 15(14):3047–3055. <https://doi.org/10.1039/c5lc00277j>
- Leturmy P, Robin C (2010) Tectonic and stratigraphic evolution of Zagros and Makran during the mesozoic-cenozoic: introduction. *Geol Soc Lond Spec Publ* 330:1–4. <https://doi.org/10.1144/SP330.1>
- Li T, Wang R, Wang Z, Zhao M, Li L (2018) Prediction of fracture density using genetic algorithm support vector machine based on acoustic logging data. *Geophysics* 83(2):D49–60
- Lyu W, Zeng L, Liu Z, Liu G, Zu K (2016) Fracture responses of conventional logs in tight-oil sandstones: a case study of the upper triassic Yanchang formation in southwest Ordos Basin, China. *AAPG Bull* 100(9):1399–1417. <https://doi.org/10.1306/04041615129>
- Malekzadeh H, Daraei M, Bayet-Goll A (2020) Field-scale reservoir zonation of the Albian-Turonian Sarvak formation within the regional-scale geologic framework: a case from the dezful embayment SW Iran. *Mar Petrol Geol* 121:104586
- Milad B, Slatt R (2018) Impact of lithofacies variations and structural changes on natural fracture distributions. *Interpretation*. <https://doi.org/10.1190/int-2017-0138.1>
- Moreau J, Joubert JB (2016) Glacial sedimentology interpretation from borehole image log: example from the late Ordovician deposits, Murzuq Basin (Libya). *Interpretation* 4(2):B1. <https://doi.org/10.1190/INT-2015-0161.1>
- Motiei H (1993) Stratigraphy of Zagros. Geological Survey of Iran Publication, Tehran
- Motiei H (1996) Petroleum geology of Zagros. Geological Survey of Iran, Iran
- Nelson RA (2001) Geologic analysis of naturally fractured reservoirs. Gulf Professional Publishing, Houston
- Nie X, Zou C, Pan L, Huang Z, Liu D (2013) Fracture analysis and determination of in-situ stress direction from resistivity and acoustic image logs and core data in the Wenchuan earthquake fault scientific drilling borehole-2(50–1370 m). *Tectonophysics* 593:161–171. <https://doi.org/10.1016/j.tecto.2013.03.005>
- Pakparvar S, Ghadimvand NK, Jahani D (2017) Sarvak reservoir facies characteristics in one of the South West field in Iran. *Open J Geol* 7(3):279–294. <https://doi.org/10.4236/ojg.2017.73020>
- Peters KE, Curry DJ, Kacwicz M (2012) Basin Modeling: new horizons in research and applications. AAPG, Tulsa. <https://doi.org/10.1306/H41331>
- Prioulet R, Jocker J (2009) Fracture characterization at multiple scales using borehole images, sonic logs, and walk around vertical

- seismic profile. AAPG Bull 93(11):1503–1516. <https://doi.org/10.1306/08250909019>
- Rider H (2002) The geological interpretation of well logs. Rider-French Consulting Sutherland, Scotland
- Saadatinejad MR, Sarkarinejad K (2011) Application of the spectral decomposition technique for characterizing reservoir extensional system in the Abadan plain, southwestern Iran. *Mar Pet Geol* 28(6):1205–1217
- Sadeq QM, Yusoff WIBW (2015) Porosity and permeability analysis from well logs and core in fracture, vugy and intercrystalline carbonate reservoirs. *J Aquac Res Dev*. <https://doi.org/10.4172/2155-9546.1000371>
- Saedi G, Soleimani B, Esmailzadeh S (2017) Fracture characterization utilizing FMI, velocity deviation logs, core description and thin sections data. *Neues Jahrbuch Für Geologie Und Paläontologie-Abhandlungen*. <https://doi.org/10.1127/njgpa/2017/0643>
- Schlumberger Educational Services (2004) FMI full-bore formation micro imager. Schlumberger WTA Marketing, Houston, pp 2
- Serra O (1989) Formation micro scanner image interpretation. Schlumberger Education Services, Houston
- Serra O, Serra L (2004) Well logging: data acquisition and applications. France, N.P. <https://www.osti.gov/etdweb/biblio/20559043>
- Shafiei A, Zendejboudi S, Dusseault M, Chatzis I (2013) Mathematical model for steamflooding naturally fractured carbonate reservoirs. *Ind Eng Chem Res* 52(23):7993–8008. <https://doi.org/10.1021/ie302791a>
- Shafiei A, Dusseault MB, Kosari E, N. Taleghani M (2018) Natural fractures characterization and in situ stresses inference in a carbonate reservoir—an integrated approach. *Energies* 11(2):312. <https://doi.org/10.3390/en11020312>
- Shakeri A, Parham S (2013) Reservoir characterization and quality controlling factors of the Fahliyan formation located in southwest Iran. *J Sci Islam Repub Iran* 24(2):135–148
- Soleimani B, Bahadori A, Meng F (2013) Micro biostratigraphy, microfacies and sequence stratigraphy of upper cretaceous and Paleogene sediments, Hendijan oilfield, Northwest of Persian Gulf, Iran. *Nat Sci* 5(11):1165–1182. <https://doi.org/10.4236/ns.2013.511143>
- Tabatabaei SME, Kadkhodaie-Ilkhchi A, Hosseini Z, Moghaddam AA (2015) A hybrid stochastic-gradient optimization to estimating total organic carbon from petrophysical data: a case study from the Ahwaz oilfield, SW Iran. *J Petrol Sci Eng* 127:35–43. <https://doi.org/10.1016/j.petrol.2015.01.028>
- Taherdangkoo R, Abdideh M (2016) Fracture density estimation from well logs data using regression analysis: validation based on image logs (case study: South West Iran). *Int J Petrol Eng* 2(4):289–301
- Tokhmchi B, Memarian H, Rezaee MR (2010) Estimation of the fracture density in fractured zones using petrophysical logs. *J Petrol Sci Eng* 72(1–2):206–213
- Ullah J, Luo M, Ashraf U, Pan H, Anees A, Li D, Ali M, Ali J (2022) Evaluation of the geothermal parameters to decipher the thermal structure of the upper crust of the Longmenshan fault zone derived from borehole data. *Geothermics* 98:102268
- Voorn M, Exner U, Barnhoorn A, Baud P, Reuschlé T (2015) Porosity, permeability and 3D fracture network characterization of dolomite reservoir rock samples. *J Petrol Sci Eng* 127:270–285. <https://doi.org/10.1016/j.petrol.2014.12.019>
- Wang J, Song H, Wang Y (2020) Investigation on the micro-flow mechanism of enhanced oil recovery by low-salinity water flooding in carbonate reservoir. *Fuel* 266:117156
- Wilson ME, Lewis D, Holland D, Hombo L, Goldberg A (2013) Development of a Papua new Guinean onshore carbonate reservoir: a comparative borehole image (FMI) and petrographic evaluation. *Mar Pet Geol* 44:164–195. <https://doi.org/10.1016/j.marpetgeo.2013.02.018>
- Yang H, Pan H, Wu A, Luo M, Konaté AA, Meng Q (2017) Application of well logs integration and wavelet transform to improve fracture zones detection in metamorphic rocks. *J Petrol Sci Eng* 157:716–723
- Zadeh PG, Adabi MH, Sadeghi A (2019) Microfacies, geochemistry and sequence stratigraphy of the Sarvak formation (Mid Cretaceous) in the Kuh-e Siah and Kuh-e Mond, Fars area, southern Iran. *J Afr Earth Sci* 160:103634. <https://doi.org/10.1016/j.jafrearsci.2019.103634>
- Zahmatkesh I, Aghli G, Mohamadian R (1994) Systematic fractures analysis using image logs and complementary methods in the Marun Oilfield SW Iran. *J Geopersia* 5(2):139–150
- Zaremoayedi F, Ghaedi M, Kazemi N (2022) A new approach to production data analysis of non-volumetric naturally fractured gas condensate reservoirs. *J Nat Gas Sci Eng* 105:104703

Publisher's Note Springer Nature remains neutral with regard to jurisdictional claims in published maps and institutional affiliations.